EMBO Molecular Medicine

Absence of Runx3 expression in normal gastrointestinal epithelium calls into question its tumour suppressor function

*Ditsa Levanon[1], Yael Bernstein[1], Varda Negreanu[1], Karen Rae Bone[1], Amir Pozner[1], Raya Eilam[2], Joseph Lotem[1], Ori Brenner[2], Yoram Groner[1]**

Keywords: colorectal cancer; epithelial expression; gastric cancer; Runx3 transcription factor; tumour suppressor gene

DOI 10.1002/emmm.201100168

Received May 11, 2011
Revised July 07, 2011
Accepted July 18, 2011

The Runx3 transcription factor regulates cell fate decisions during embryonic development and in adults. It was previously reported that Runx3 is strongly expressed in embryonic and adult gastrointestinal tract (GIT) epithelium (Ep) and that its loss causes gastric cancer. More than 280 publications have based their research on these findings and concluded that *Runx3* is indeed a tumour suppressor (TS). In stark contrast, using various measures, we found that Runx3 expression is undetectable in GIT Ep. Employing a variety of biochemical and genetic techniques, including analysis of Runx3-GFP and R26LacZ/Runx3^{Cre} or R26tdTomato/Runx3^{Cre} reporter strains, we readily detected Runx3 in GIT-embedded leukocytes, dorsal root ganglia, skeletal elements and hair follicles. However, none of these approaches revealed detectable Runx3 levels in GIT Ep. Moreover, our analysis of the original Runx3$^{LacZ/LacZ}$ mice used in the previously reported study failed to reproduce the GIT expression of Runx3. The lack of evidence for Runx3 expression in normal GIT Ep creates a serious challenge to the published data and undermines the notion that Runx3 is a TS involved in cancer pathogenesis.

INTRODUCTION

Runx3 is one of the three mammalian Runt domain transcription factors (TFs; Runx1, Runx2 and Runx3) comprising the highly conserved *RUNX* gene family. Runx TFs are key gene expression regulators of cell proliferation and lineage commitment during embryonic development and in adults. *Runx3* was originally cloned based on its similarity to *Runx1* (Levanon et al, 1994) and subsequently localized on human and mouse chromosomes 1 and 4, respectively (Avraham et al, 1995; Levanon et al, 1994). Tissue-specific Runx3 expression is transcriptionally regulated by two alternative control regions, designated the distal (P1) and proximal (P2) promoters (Fig 1A; Bangsow et al, 2001; Levanon & Groner, 2004).

(1) Department of Molecular Genetics, The Weizmann Institute of Science, Rehovot, Israel
(2) Department of Veterinary Resources, The Weizmann Institute of Science, Rehovot, Israel
***Corresponding author:** Tel: +972-8-9343972, Fax: +972-8-9344108; E-mail: yoram.groner@weizmann.ac.il

We previously published a detailed survey of the spatio-temporal expression of Runx3 during embryonic development (Levanon et al, 2001). Runx3 expression was examined at embryonic day (E) 10.5 and between E14.5 and E16.5, and compared to the expression pattern of Runx1. Immunohistochemistry (IHC) and knock-in (KI) β-galactosidase activity (LacZ staining) were used in parallel throughout this analysis to rigorously determine the expression patterns of the two TFs. Runx3 and Runx1 were readily detected in different compartments of the haematopoietic system and also in the dorsal root ganglia (DRG), epidermal appendages and developing skeletal elements (Levanon et al, 2001). However, regarding epithelia an interesting distinction was noted in the expression pattern of Runx1 and Runx3. While Runx1 was expressed in various epithelia including mucosa of the oesophagus and stomach, the salivary glands ducts and the olfactory and respiratory mucosa, Runx3 expression was undetectable in these epithelia (Levanon et al, 2001).

Subsequently, Li et al (Li et al, 2002) reported that Runx3 is highly expressed in GIT epithelial cells of E14.5 embryo and adult mice and that its loss causes gastric cancer. In their study,

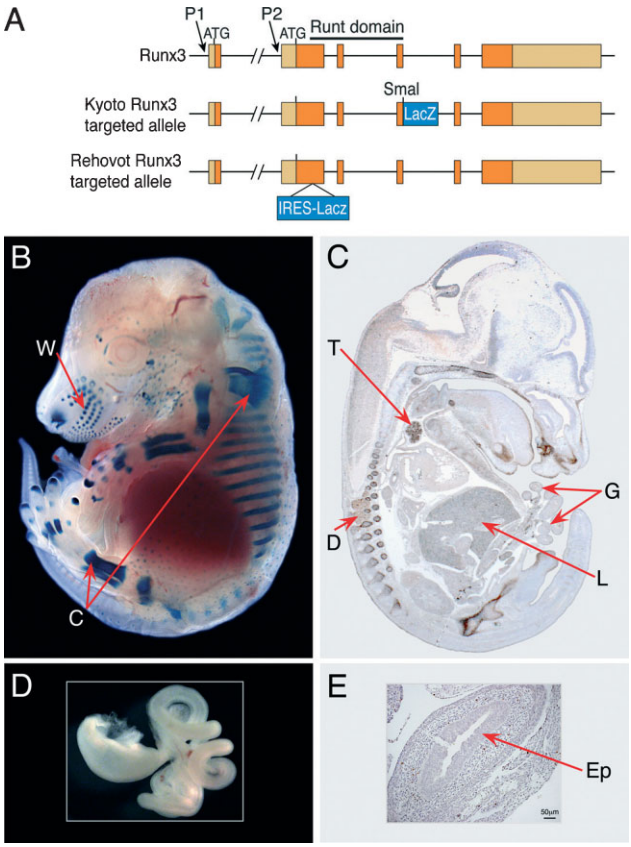

Figure 1. Detection of Runx3 in WT and in Rehovot-Runx3$^{Lacz/+}$ mice.

A. Scheme depicting the *Runx3* gene and the targeted alleles used to generate the Kyoto- and Rehovot- Runx3$^{LacZ/LacZ}$ mice. The two promoters (P1 and P2) and the corresponding initiator ATGs are indicated. In Kyoto-Runx3$^{LacZ/LacZ}$ mice, the LacZ was inserted in frame into exon 4 of the gene creating a Runx3-LacZ fusion protein (Li et al, 2002). In Rehovot- Runx3$^{LacZ/LacZ}$ mice, the gene was disrupted by inserting an IRES-LacZ into exon 2 (Levanon et al, 2002).

B,C. The pattern of Runx3 expression at E14.5 revealed by whole mount LacZ staining of Rehovot-Runx3$^{LacZ/+}$ embryo (B) and by IHC of WT embryo using a sagittal section reacted with Poly-G Ab (C). Runx3 is strongly expressed in whiskers (**W**), cartilage (**C**), thymus (**T**), DRG (**D**) and haematopoietic cells in the liver (**L**), but not in the GIT (**G**).

D,E. Isolated LacZ-stained GIT of E14.5 Runx3$^{LacZ/+}$ embryo (D) and a transverse section of the intestine of a WT embryo (E) immunostained with poly-G Abs showing lack of detectable Runx3 in the epithelium (Ep).

these authors used mice in which the β-gal gene was knocked into the Runx3 locus, enabling Runx3 expression to be monitored by visualizing LacZ staining. In describing their study, Li et al state that 'Strong β-gal activity was found in gastrointestinal organs, including the stomach and the small and large intestines, from 14.5 dpc through to adulthood'. This statement was based on the finding that the GIT of their Runx3$^{LacZ/LacZ}$ knockout (KO) embryos was darkly stained by LacZ, in striking contrast to the wild-type (WT) GIT. Many investigators considered Li's data (Li et al, 2002) and conclusion that loss of Runx3 was involved in genesis of cancer, convincing enough to launch studies on the potential involvement of Runx3 in additional types of carcinoma. Theses studies involved a wide spectrum of tumours including bladder, brain, breast, colorectal, liver, lung, pancreas and prostate (Table S1 of Supporting information lists 286 publications addressing association of Runx3 loss with various cancers). Of note, the majority of these published papers report Runx3 promoter methylation taken as an indication for loss of Runx3 expression.

Clearly, the data reported by Li et al (Li et al, 2002) did not correspond with our previously described findings regarding Runx3 expression in GIT epithelium (Ep). However, given the stringency of combined IHC and LacZ analysis that we had employed (Levanon et al, 2001), it was not clear how we could have missed such strong expression in a major organ, particularly since all other LacZ-expressing sites shown in Li et al corresponded with those reported previously by our own group (Levanon et al, 2002, 2001). The use of LacZ KI reporter to monitor expression is usually a reliable and highly sensitive technique for determining gene expression levels. Therefore, in light of these contradictory results, we concluded that the issue of Runx3 expression in the normal GIT Ep needed to be revisited.

In an attempt to resolve the discrepancy between Li's report and our results, we suggested at the time (Levanon et al, 2003) the possibility that the positive detection of Runx3 in GIT by Li et al was due to an artefact caused by the structure of the targeting constructs used for creating the Runx3$^{LacZ/+}$ mouse strains (Levanon et al, 2002, 2001; Li et al, 2002). Li et al (Li et al, 2002) used a KO mouse (hereafter referred to as Kyoto-Runx3$^{Lacz/LacZ}$), in which the LacZ-neomycin (*neo*) cassette was inserted in-frame into exon 4 of the *Runx3* gene, creating a Runx3-LacZ fusion protein (Fig 1A). In contrast, we (Levanon et al, 2001) used Runx3 KO mice (hereafter referred to as Rehovot-Runx3$^{Lacz/LacZ}$) in which *Runx3* was disrupted by inserting an IRES-LacZ-*neo* cassette into exon 2 (Levanon et al, 2002). In the Rehovot-Runx3$^{Lacz/LacZ}$ mice, expression of LacZ is enabled by the presence of an IRES segment, which results in the production of free LacZ protein (Fig 1A). Accordingly, it seemed possible that the genetic manipulations used for preparation of either of these mouse strains might have caused a change in the expression pattern. However, the differences between the targeted alleles of these Runx3$^{Lacz/LacZ}$ mouse strains, as shown here, do not reconcile the discrepancies in the published findings.

Responding to these issues, we re-examined Runx3 expression in normal GIT Ep using a variety of biochemical and genetic techniques including IHC with eight different anti-Runx3 antibodies (Abs), ^{35}S-RNA *in situ* hybridization (RISH), TaqMan reverse transcription quantitative real-time polymerase chain reaction (RT-qPCR) of FACS sorted GIT epithelial cells, analysis of Runx3-GFP KI mice, analysis of R26-LacZ/Runx3^{Cre} and R26-tdTomato/Runx3^{Cre} mice and rigorous re-analysis of the original Kyoto-Runx3$^{Lacz/LacZ}$ mice used by Li et al (Li et al, 2002). This exhaustive analysis revealed no expression of Runx3 in GIT Ep and, therefore, poses a serious challenge to the published data and to the conclusion that *Runx3* is a tumour suppressor gene (TSG) whose inactivation is involved in gastric or colorectal cancer. Of note, the detailed analysis documented herewith demonstrated that of the various anti-Runx3 Abs used for

detection of Runx3 in GIT Ep, the widely used subtype designated R3-1E10 (Ito et al, 2009) is an invalid reagent and could not be construed as being specific for Runx3 protein. Given the lack of Runx3 expression in a wide repertoire of other epithelia, the data also calls into question the potential function of Runx3 as TSG in other carcinomas. It is commonly accepted that if a gene is never expressed in a cell type that gives rise to a particular tumour, loss of its expression in that tissue cannot be invoked to mechanistically explain the pathogenesis of such tumours in that tissue.

RESULTS AND DISCUSSION

Analysis of tissue-specific expression of Runx3 by IHC and LacZ staining

We first repeated the detailed analysis of Runx3 expression at E14.5 using combined whole mount LacZ staining (Rehovot-Runx3$^{Lacz/+}$) and IHC of sagittal sections with our original (Levanon et al, 2001) anti-Runx3 polyclonal Ab, Poly-G (Fig 1B–E). While these experiments yielded consistent results that corresponded with the known phenotypic features of Runx3$^{-/-}$ mice (Levanon & Groner, 2009), they failed to reveal the pronounced Runx3 expression in GIT Ep reported by Li et al (Li et al, 2002). Next, we assessed Runx3 expression in embryos and adult mice by IHC using four additional anti-Runx3 monoclonal or polyclonal Abs that were raised against various regions of the protein, either by us or by others (Fig 2A). Polyclonal anti-Runx3-Poly-SA was raised against a region of Runx3 similar to that of anti-Runx3 Poly-G. The other three Abs designated Pep-J, GS and Mono-G were raised against peptides spanning Runx3 regions previously defined by Ito et al (Ito, 2008) as being 'exposed in the GIT' (Fig S1 A–C of Supporting information and Supporting information text: Evaluation of anti-Runx3 Abs reliability). Of note, the analyses using all five Abs (Fig 2A) failed to detect Runx3 in the GIT Ep (Fig 2B–F) even though they readily detected Runx3 in other cell types in the same or adjacent tissues, such as GIT-embedded leukocytes (in the adult GIT) and the DRG neurons of embryos (Fig 2B–F).

More recently, the group of Yoshiaki Ito (the corresponding author of Li et al, 2002) raised several new monoclonal anti-Runx3 Abs (Ito et al, 2009) one of which (designated R3-1E10) was used in their reports. We have evaluated three of those anti-Runx3 Abs: R3-8C9, R3-3F12 and R3-1E10. R3-8C9 and R3-3F12 reacted with Runx3 in DRG and leukocytes, whereas, R3-1E10 did not (Fig S1B and C of Supporting information and Supporting information text: Evaluation of anti-Runx3 Abs reliability). Using R3-1E10 Abs on sections of either DRG or GIT tissues, we confirmed the finding of Ito et al (Ito et al, 2009) that

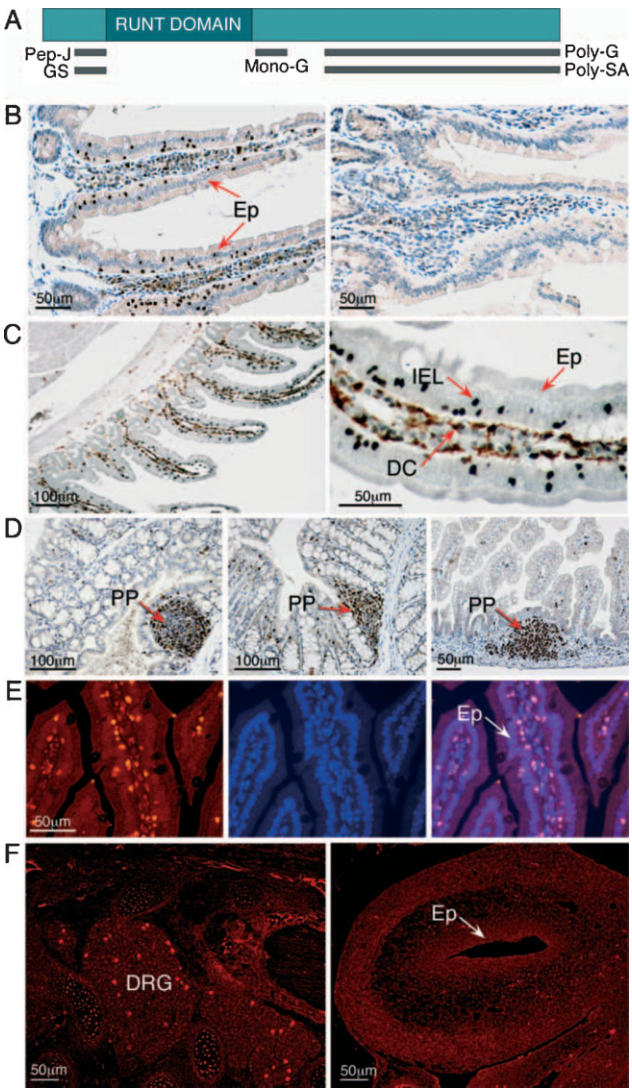

Figure 2. Five different anti-Runx3 Abs fail to detect Runx3 in GIT epithelium (Ep).

A. Scheme showing Runx3 protein structure indicating the position of peptides used for generation of the five anti-Runx3 Abs (see Materials and Methods Section for details). Poly-G, Poly-SA-, Pep-J and GS are rabbit polyclonal Abs. Mono-G is a monoclonal Ab.

B. Transverse sections of adult WT (left) and Runx3$^{-/-}$ (right) small intestine immunostained with the Poly-G Ab. Runx3 was detected in WT GIT-embedded leukocytes (left) but not in Runx3$^{-/-}$ cells. No Runx3 was detected in WT GIT Ep.

C. Transverse sections of the small intestine of an adult CX3CR1$^{GFP/+}$ mouse (Jung et al, 2000) double-stained with Poly-G and anti-GFP Abs. In adult GIT, Runx3 is expressed in dendritic cells (DCs) and intraepithelial leukocytes (IEL). CX3CR1^{GFP} marks the GIT DCs. Runx3 was detected in GIT IEL (black nuclear staining, see arrows in the enlarged right panel). Double stained Runx3/GFP positive (brown cell membrane staining) depicts Runx3 expressing DCs. No Runx3 was detected in GIT Ep.

D. Three distinct anti-Runx3 Abs (From left to right: Poly-G, Poly-SA and Pep-J) detected Runx3 in small intestine Peyer's patch (PP) and leukocytes of adult mice, but not in GIT Ep.

E. Adult WT small intestine immunostained with Mono-G anti-Runx3 Ab (left panel) and with 4′-6-diamidino-2-phenylindole (DAPI) which stains the nuclei of both leukocytes and epithelial cells (middle panel) and a merged image of the two frames (right panel) revealing Runx3 expression in GIT-embeded IEL, but not in the Ep.

F. In E14.5 WT embryos Mono-G Abs detected Runx3 in DRG (left) but not in GIT (right). More details are presented in Fig S1 of Supporting information and in Supporting information text: evaluation of anti Runx3 Abs).

R3-1E10 does not react with DRG, but additionally we found that it did not react with either GIT epithelial cells or with the GIT-embedded leukocytes (Fig S1C of Supporting information). Of note, the inability of R3-1E10 to detect Runx3 in DRG and/or in leukocytes, the two major and undisputed sites of Runx3 expression, disqualifies it as a valid anti-Runx3 Ab. Supporting this conclusion are the findings that the Mono-G Ab, which was raised against the same GIT Ep 'exposed' region (Fig S1A of Supporting information), readily reacted with Runx3 in GIT-embedded leukocytes and DRG (Fig S1B and C of Supporting information). Hence, results attained using R3-1E10 Ab should be interpreted cautiously, particularly when its reaction with GIT Ep serves as the sole evidence for Runx3 expression in that tissue (Ito et al, 2008).

Regarding detection of Runx3 by IHC, it is important to note that of the eight anti-Runx3 Abs (including R3-8C9 and R3-F12) that we have tested, not a single one produced a reliable Runx3 signal when reacted with GIT Ep (Fig 2 and Figs S1 and S2 of Supporting information). However, all these Abs readily reacted with Runx3 in DRG and leukocytes. Given that GIT epithelial cells are notorious for their high degree of non-specific Ab binding, these findings pose a serious challenge to published data detecting Runx3 in GIT Ep solely by IHC. The data below demonstrating by various measures that Runx3 expression in undetectable in GIT Ep strongly supports this conclusion.

As noted above, since the publication of the Li et al (2002) paper, a rich literature has been published on the potential involvement of Runx3 in a variety of cancers (Table S1 of Supporting information). While the majority of these published papers report *Runx3* promoter methylation in human cancers as an indication for loss of Runx3 expression, few also analyse Runx3 expression by IHC. We thus evaluated RUNX3 expression in normal human GIT Ep. Sections of cardio-pyloric stomach were immunostained with two highly specific anti-RUNX3 Abs as compared to pre-immune serum (Fig S2 of Supporting information). RUNX3 protein was clearly detected in the tissue-embedded leukocytes, but not in the Ep (Fig S2 of Supporting information). Thus, similar to our findings in the mouse GIT, RUNX3 is undetectable in human gastric Ep.

Runx1, a member of the same TF family as Runx3, is readily detected in GIT epithelium by IHC, LacZ staining and ^{35}S-RNA *in situ* hybridization

In contrast to our inability to detect Runx3 expression in GIT Ep, we previously detected the expression of the RUNX family member Runx1 in GIT Ep (Levanon et al, 2001). This epithelial expression was also re-examined here using both IHC with anti-Runx1 Abs and LacZ staining of Runx1$^{LacZ/+}$ mice (North et al, 1999). As shown in Fig 3A and B, Runx1 was readily detected in GIT Ep. Moreover, the intensity of immunostaining in GIT Ep (Fig 3A) correlated well with that of the whole mount LacZ staining (Fig 3B).

We used the expression of Runx1 as a control to evaluate GIT expression of Runx3 by ^{35}S-RISH. Both Runx3 and Runx1 are expressed in DRG (Levanon et al, 2001), but in different classes of neurons; Runx3 is expressed in TrkC neurons, whereas,

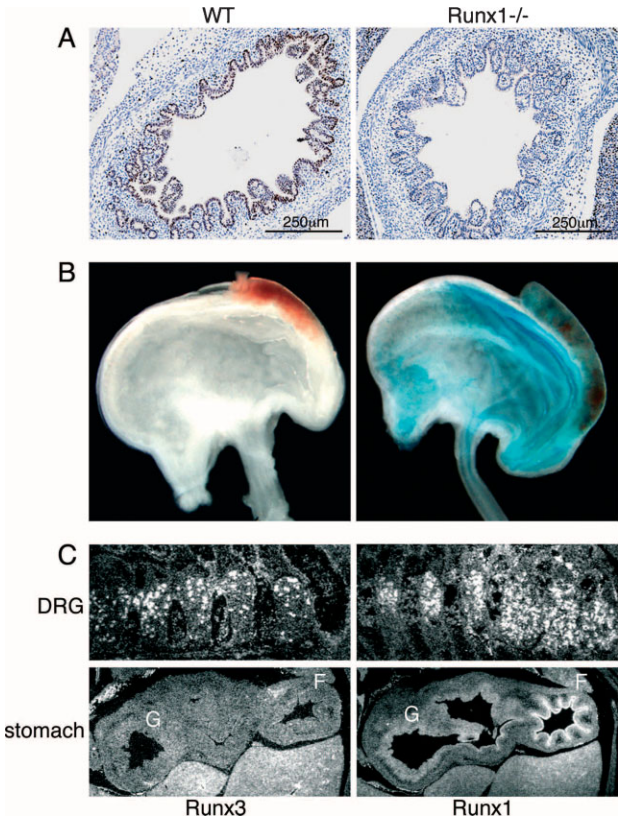

Figure 3. Expression of Runx1, a fellow family member of Runx3, is easily detected in GIT epithelium (Ep).

A. Sections of E16.5 forestomach of WT and Runx1-P2$^{Neo/Neo}$ embryos immunostained with anti-Runx1 Ab show Runx1 expression in WT but not in the negative control Runx1-P2$^{Neo/Neo}$ forestomach (adapted from Pozner et al, 2007).

B. Whole mount LacZ stained stomach of WT (left) and Runx1$^{LacZ/+}$ (right) E14.5 embryos. LacZ staining was more prominent in the forestomach.

C. ^{35}S-RNA *in situ* hybridization analysis of *Runx1* and *Runx3* expression in embryonic DRG and stomach. DRG and stomach of E16.5 WT embryos were hybridized with a Runx3 probe (left panels) and a Runx1 probe (right panels). Both probes detected expression in the DRG (Runx1 in TrkA neurons and Runx3 in TrkC neurons), but only the Runx1 probe detected expression in gastric Ep. F, forestomach, G, glandular stomach (adapted from Brenner et al, 2004).

Runx1 is expressed in TrkA neurons (Chen et al, 2006; Kramer et al, 2006; Levanon et al, 2002). Analysis of WT embryos using ^{35}S-labelled probes revealed *Runx3*-^{35}S-RISH signals in DRG but not in gastric Ep, whereas, *Runx1* was detected in both organs (Fig 3C). *Runx1* signals were high in the fore-stomach and lower in the glandular stomach region.

Collectively, these expression results of Runx3 and Runx1 demonstrated that while Runx1 was clearly detectable in GIT Ep, Runx3 could not be detected. Accordingly, the conclusion that Runx3 (both mRNA and protein) is absent in GIT Ep was confirmed by the results of three straightforward and sensitive procedures: LacZ staining, IHC (with several Abs) and ^{35}S-RISH, which were used in parallel to assay the expression of Runx1 and Runx3.

Analysis of Runx3-GFP reporter mice failed to detect GFP-positive GIT epithelial cells

One alternative to the use of a LacZ reporter is the widely used green fluorescent protein (GFP) reporter gene. Its high expression level, when encoded as a non-fused protein, and its inherent stability make it an invaluable tool for recording spatial and temporal patterns of gene expression *in vivo*. In order to further evaluate the GIT epithelial expression of Runx3, we generated KI mice in which the GFP variants AFP or EGFP were placed downstream of the *Runx3* P1 or P2 initiator ATG, respectively (Fig 4A). These Runx3$^{P1\text{-}AFP/+}$ and Runx3$^{P2\text{-}EGFP/+}$ mice were mated to create compound heterozygous (Runx3$^{P1\text{-}AFP/P2\text{-}EGFP}$) mice.

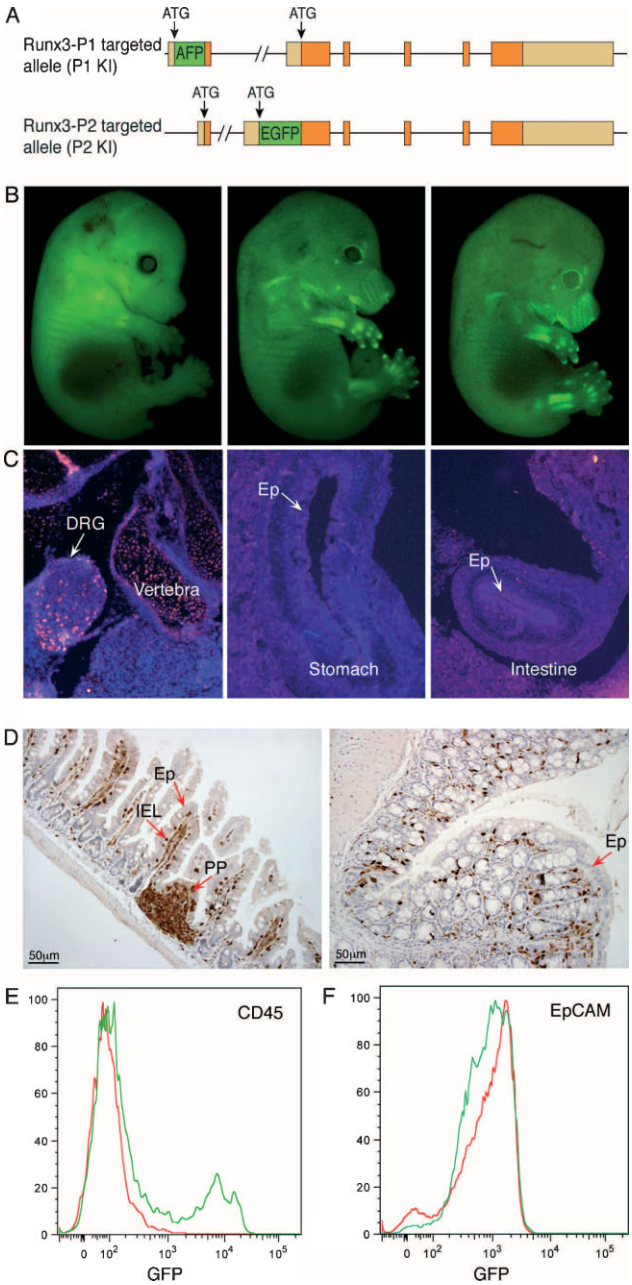

We found that the GFP expression pattern of E14.5 Runx3$^{P1\text{-}AFP/P2\text{-}EGFP}$ mice recapitulated the pattern of Runx3 expression obtained using LacZ and/or IHC (Fig 1B and C and Levanon et al, 2002, 2001), including expression in the DRG, skeletal elements and epidermal appendages (Fig 4B). To analyse GFP expression in GIT Ep in a more stringent manner, we took advantage of the commercial high avidity anti-GFP Ab to detect Runx3 by IHC. Immunostained sections of the E14.5 embryos showed intense signals in DRG and vertebrae, but none in the GIT Ep (Fig 4C). We also used the anti-GFP Ab to immunostain GIT of adult mice (Fig 4D). In this case as well, Runx3 expression was detected in GIT-embedded leukocytes, but not in GIT Ep within the same section (Fig 4D). These results, demonstrating the lack of Runx3 expression in GIT Ep of Runx3-GFP mice, correspond with the LacZ, IHC and ^{35}S-RISH results shown above.

We then assessed Runx3 expression in GIT epithelial cells of adult Runx3$^{P1\text{-}AFP/P2\text{-}EGFP}$ mice by flow cytometric analysis of GFP expressing cells. We utilized the expression of Runx3 in GIT IEL (Fig 2B–E) as a control to evaluate Runx3 expression in the epithelial cells. Single-cell suspensions were prepared from the intestine of adult Runx3$^{P1\text{-}AFP/P2\text{-}EGFP}$ mice, and GFP expression was simultaneously monitored in EpCAM$^+$ epithelial cells and CD45$^+$ IEL (Fig 4E and F). Even though the relative abundance of IEL in GIT Ep cell-suspensions is low compared to the epithelial cells, CD45$^+$/GFP$^+$ double-positive cells were readily detected (Fig 4E), whereas, there were no GFP signals associated with the EpCAM$^+$ epithelial cell population (Fig 4F). These results further demonstrate that Runx3 expression in the GIT Ep was undetectable even by the highly sensitive fluorescence activated cell sorter (FACS) analysis.

Figure 4. Analysis of Runx3 expression in Runx3$^{P1\text{-}AFP/P2\text{-}GFP}$ compound KI mice.

A. A scheme of the P1-AFP and P2-EGFP targeted alleles used to generate the Runx3-GFP reporter mice.

B. Whole mount view of Runx3$^{P1\text{-}AFP/+}$, Runx3$^{P1\text{-}AFP/P2\text{-}GFP}$ and Runx3$^{P2\text{-}GFP/+}$ (from left to right) E14.5 embryos.

C. Sagittal sections of DRG and GIT of E14.5 Runx3$^{P1\text{-}AFP/P2\text{-}GFP}$ embryos immunostained with anti-GFP Abs. GFP was detected in DRG and vertebrae, but not in gastric and intestinal epithelium (Ep).

D. Sections of adult Runx3$^{P1\text{-}AFP/P2\text{-}GFP}$ GIT (small intestine, left; colon, right) immunostained with anti-GFP Abs show GFP positive leukocytes in Peyer's patch (PP) and IEL and in leukocytes within the lamina propria, while the adjacent Ep is unstained.

E,F. Flow cytometric analysis of GFP expression in single cell-suspensions of GIT Ep of adult Runx3$^{P1\text{-}AFP/P2\text{-}GFP}$ mice. Histograms demonstrating EGFP/AFP expression in CD45$^+$ IEL (E) or EpCAM$^+$ epithelial cells (F) of Runx3$^{P1\text{-}AFP/P2\text{-}GFP}$ GIT (green) compared to WT (red). No GFP positive GIT epithelial cells (F) were detected. Results from one of four Runx3$^{P1\text{-}AFP/P2\text{-}GFP}$ and WT control mice with the same findings are shown. The relative high mean fluorescence intensity of both Runx3$^{P1\text{-}AFP/P2\text{-}GFP}$ and WT GIT epithelial cells was due to the known autofluorescence of epithelial cells (DaCosta et al, 2005).

Analyses of ROSA26-LacZ/Runx3^{Cre} and R26-tdTomato/Runx3^{Cre} mouse strains provide further evidence for lack of Runx3 expression in GIT epithelium

To further explore Runx3 expression in WT mice, we used Cre recombinase reporter strains harbouring either the LacZ or tdTomato gene within the ROSA26 locus (R26; Soriano, 1999; Srinivas et al, 2001 and Materials and Methods Section). These strains display amplified expression of LacZ or tdTomato following Cre-mediated excision of loxP-flanked (Floxed) transcriptional 'stop' sequences (Soriano, 1999; Srinivas et al, 2001). To faithfully replicate the native Runx3 expression pattern, we generated Runx3-Cre KI mice (Runx3^{Cre}) harbouring a GFP-Cre cassette in *Runx3* exon 4 (Fig 5A). Of note, the cassette was inserted in-frame into the unique *SmaI* site, which was originally used to generate the Kyoto-Runx3^{LacZ}/^{LacZ} mice (see Materials and Methods Section). Thus, the expression of Cre in this Runx3^{Cre} mouse strain recapitulates the LacZ expression mode of the Kyoto-Runx3^{LacZ}/^{LacZ} mice (Li et al, 2002). Upon crossing Runx3^{Cre} mice into R26-stop^{Floxed}-LacZ or R26-stop^{Floxed}-tdTomato mice, the reporter (*i.e.* LacZ or tdTomato) is switched on in all cells expressing Runx3 and from then on constitutively expressed within the R26 locus. This occurrence generates a permanent genetic mark, which is transmitted to all progeny cells allowing to trace not only constant but also transient expression of Runx3 even in rare cell populations. When E14.5 R26-LacZ/Runx3^{Cre} or R26-tdTomato/Runx3^{Cre} embryos were analysed, we found no sign of Runx3 expression in GIT Ep (Fig 5B, C and F), in striking contrast to the intense Runx3^{Cre}-mediated expression in all other Runx3-expressing organs (Levanon et al, 2002, 2001; Li et al, 2002; Fig 5B and F, also see Fig 1). The undetectable expression of LacZ or tdTomato in normal GIT Ep precludes the possibility that Runx3 is expressed in small progenitor compartments of epithelial cells.

We then used the R26-LacZ/Runx3^{Cre} or R26-tdTomato/Runx3^{Cre} mice to assess Runx3 expression in embryonic GIT Ep by flow cytometric analysis. For LacZ analysis, we employed fluorescein di-β-D-galactopyranoside (FDG), one of the most sensitive fluorogenic substrates available for detecting β-galactosidase. As Runx3 was previously detected in the thymus and liver of the developing embryo (Collins et al, 2009; Levanon et al, 2001; Woolf et al, 2003; GenePaint.org http://www.genepaint.org/Frameset.html, and Fig 1C and 5B), we used the expression of Runx3 in thymocytes as a control to evaluate its expression in the GIT. Single-cell suspensions were prepared from the thymus and GIT of E16.5 WT and R26-LacZ/Runx3^{Cre} embryos, and LacZ (FDG) was simultaneously monitored in epithelial cells and thymocytes (Fig 5D and E). While CD45$^+$/FDG$^+$ double-positive cells were readily detected in the thymocytes (Fig 5D), no FDG signals were associated with the EpCAM$^+$ epithelial cell population (Fig 5E).

We next assessed Runx3 expression in GIT epithelial cells by flow cytometric analysis of tdTomato$^+$ epithelial cells of R26-tdTomato/Runx3^{Cre} mice (Fig 5G and H). Taking advantage of the intensively fluorescent tdTomato protein, we show that as with LacZ, E16.5 thymocytes co-expressed CD45 and tdTomato whereas EpCAM$^+$ cells did not express tdTomato (Fig 5G). In adults we utilized, as in Fig 4E and F, the expression of Runx3 in GIT-embedded IEL as a control for Runx3 expression in the epithelial cells. Single-cell suspensions were prepared from the intestine of adult R26-tdTomato/Runx3^{Cre} mice, and tdTomato was examined by FACS analysis. tdTomato was simultaneously monitored in EpCAM$^+$ epithelial cells and CD45$^+$ IEL (Fig 5H). Naturally, most of the cells in GIT Ep cell suspensions are epithelial cells, while the GIT-embedded IEL constitute a minor fraction (see Fig 2C). Moreover, Runx3 is expressed only in certain subsets (CD8+, DCs NK) of the CD45$^+$ cells as evidenced by CD45$^+$/tdTomato$^+$ double-positive cells (Fig 5H). Although Runx3$^+$ CD45$^+$ subsets differ in their level of Runx3 expression, the reporter produces an equal signal for all populations, reflecting the constitutive activity of the R26 locus. In contrast to the CD45$^+$ cells, no tdTomato signals were associated with the EpCAM$^+$ epithelial cell population, evidenced by the lack of reporter signal with R26-mediated intensity seen in CD45$^+$ cells (Fig 5H).

We next recorded the expression of Runx3 by RT-qPCR. Employing flow cytometric analysis, we isolated EpCAM$^+$CD45$^-$ epithelial cells from adult GIT and used splenic CD45$^+$NK cells as a positive control. RT-qPCR was conducted using Runx3-specific TaqMan primers. Strikingly, the expression of Runx3 in the positive control CD45$^+$NK cells was 2257 fold higher relative to the EpCAM$^+$ epithelial cells as calibrator ($p = 0.001$; Fig 5I). Of note, the CD45$^+$NK cells signal appeared at cycle 26.2, whereas, that of the EpCAM$^+$ epithelial cells arose at greater than 35 cycles (at cycle 37), more than 5 cycles higher than any other assay for an equivalent RNA input. By these standard criteria, we interpret the recorded values to mean that there is effectively no true target for Runx3 primers in WT GIT Ep.

Taken together, these results demonstrate that Runx3 expression was undetectable in embryonic and adult GIT Ep even when TaqMan RT-qPCR or the highly sensitive combination of enhanced expression of R26-LacZ or R26-tdTomato and FACS analysis was used. Importantly, the absence of FDG or tdTomato positive EpCAM cells indicates that Runx3 was not even transiently expressed at any time point during epithelial lineage development.

Rigorous analysis of the original Kyoto-Runx3$^{LacZ/LacZ}$ mice failed to reproduce the reported LacZ staining in the GIT

In a further attempt to clarify the cause of the conflicting results regarding Runx3 expression in GIT Ep, we recently obtained the Kyoto-Runx3 KO mice used in the original study of Li et al (Li et al, 2002). Male and female Kyoto-Runx3$^{LacZ/+}$ mice were mated, and their progeny was analysed at E14.5. As each pregnancy resulted in Runx3$^{+/+}$, Runx3$^{LacZ/+}$ and Runx3$^{LacZ/LacZ}$ embryos, the entire litter was first stained for LacZ and only subsequently genotyped. Based on the consensus regarding Runx3 expression in DRG and skeletal elements of E14.5 embryos (Inoue et al, 2002; Levanon et al, 2002, 2001; Li et al, 2002; Yoshida et al, 2004), the level of LacZ staining in these organs was used as a positive control reference.

Staining of either Kyoto-Runx3$^{LacZ/+}$ or Kyoto-Runx3$^{LacZ/LacZ}$ embryos revealed Runx3-LacZ expression in the DRG and skeletal elements at intensities similar to those previously observed in these mice (Li et al, 2002; Yoshida et al, 2004), yet

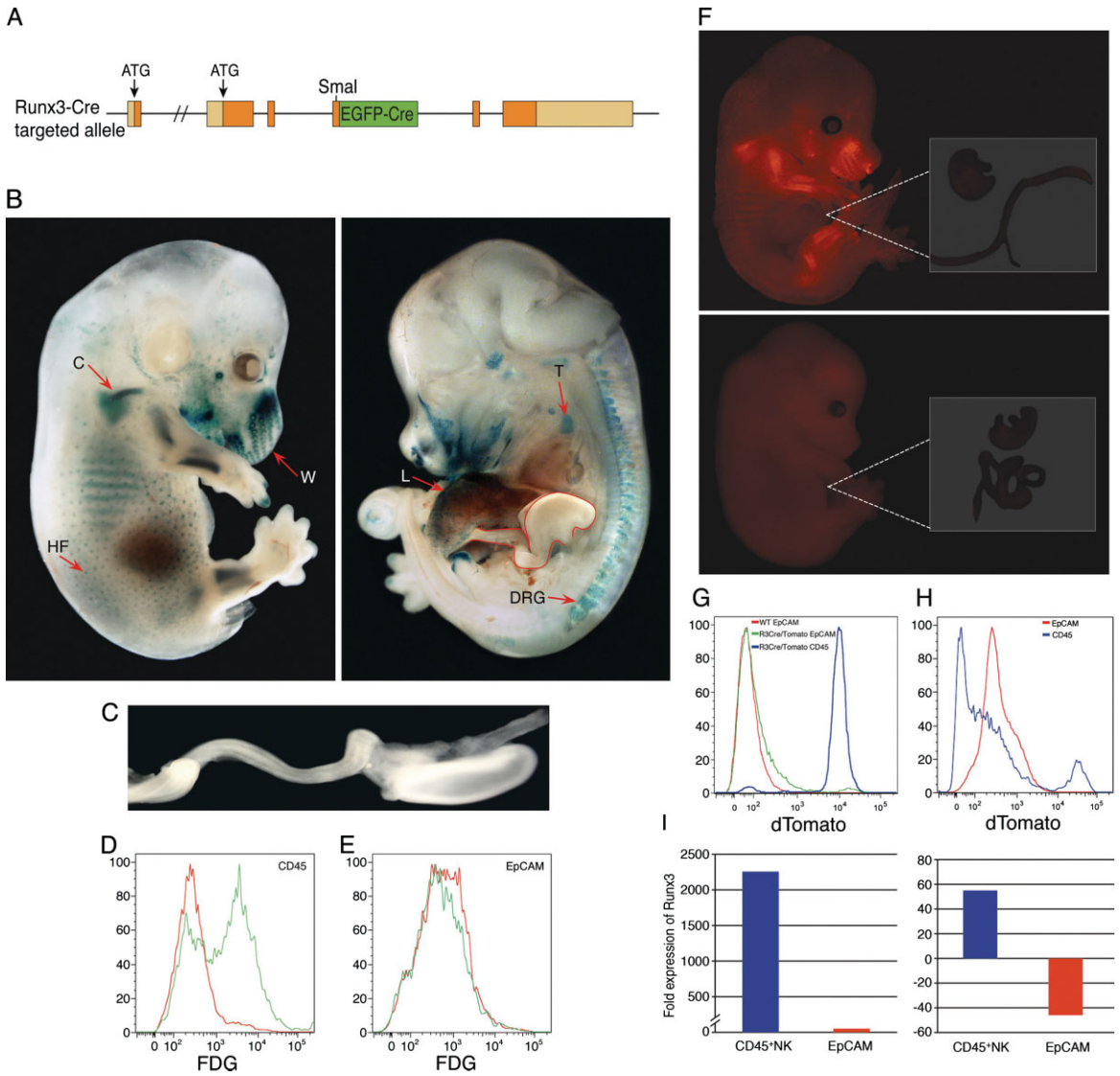

Figure 5. LacZ or tdTomato expression in R26-LacZ/Runx3-^{Cre} or R26-tdTomato/Runx3^{Cre} mice and RT-qPCR analysis of Runx3 in GIT epithelial cells.

A. Scheme of the Runx3-GFP-Cre targeted allele used to create the Runx3^{Cre} mice. The GFP-Cre cassette was inserted in frame into the *SmaI* site used for the generation of the Kyoto-Runx3$^{LacZ/LacZ}$ mice (see Fig 1A).

B,C. LacZ expression in whole mount E14.5 R26-LacZ/Runx3^{Cre} embryo. The GIT, outlined in red (right panel), was excised, stretched and is shown magnified in (C). W, whiskers; C, cartilage; T, thymus; L, liver; HF, hair follicles.

D,E. Flow cytometric analysis of Runx3 expression (FDG serves as a fluorescence substrate for β-gal) in thymocytes and GIT epithelial cells of E16.5 R26-LacZ/Runx3^{Cre} embryos. (D) Histograms demonstrating detection of CD45$^+$/FDG$^+$ double positive thymocytes (green) of R26-LacZ/Runx3^{Cre} embryo compared to WT (red). (E) Absence of FDG$^+$ cells in GIT epithelial cells of either WT (red) or R26-LacZ/Runx3^{Cre} embryos (green). Results from one of four R26-LacZ/Runx3^{Cre} and WT control embryos with same findings are shown.

F. tdTomato expression in whole mount E14.5 R26-tdTomato/Runx3^{Cre} (upper panel) or R26-tdTomato (lower panel) embryos. Red tdTomato fluorescence is seen in cartilage of skeletal elements, whiskers and hair follicles. The GIT of both R26-tdTomato/Runx3^{Cre} and R26-tdTomato embryos was excised, stretched and is shown magnified on the right.

G. Flow cytometric analysis of Runx3 expression (via tdTomato fluorescence) in thymocytes and GIT epithelial cells of E16.5 R26-tdTomato/Runx3^{Cre} embryos.

H. Flow cytometric analysis of tdTomato in single cell-suspensions of GIT epithelium (Ep) of adult R26-tdTomato/Runx3^{Cre} mice. Results from one of four adult R26-tdTomato/Runx3^{Cre} mice with same findings are shown.

I. RT-qPCR analysis of Runx3 expression in splenic NK and GIT epithelial cells of adult WT mice. cDNAs of splenic CD45$^+$ NK cells and of sorted EpCAM$^+$CD45$^-$ GIT epithelial cells were analysed with Runx3, PBGD and HPRT TaqMan assays as detailed under Materials and Methods Section. Results were normalized to endogenous control genes and calculated relative to a calibrator. Left panel. Expression of Runx3 in CD45$^+$NK cells is 2257 fold higher relative to the EpCAM$^+$ epithelial cells as calibrator ($p = 0.001$). The right panel depicts the expression of Runx3 in CD45$^+$NK cells and EpCAM$^+$CD45$^-$ epithelial cells calculated relative to the PBGD as calibrator ($p = 0.001$). Of note, signals produced by the EpCAM$^+$CD45$^-$ GIT epithelial sample were consistently detected after more than 35 cycles, 5 cycles higher than any other assay for an equivalent RNA input. By these standard criteria, we interpret the recorded values to mean there is effectively no true target for Runx3 in WT GIT Ep.

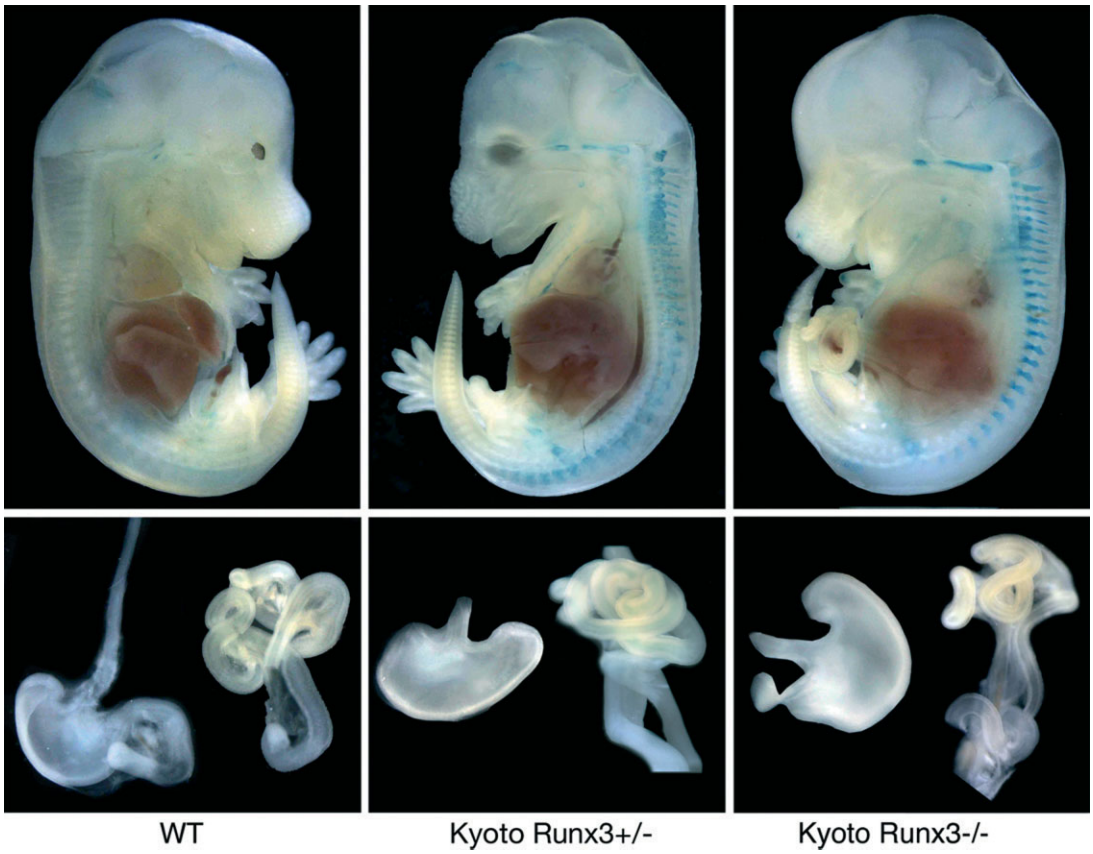

Figure 6. Absence of LacZ expression in GIT of the original Kyoto-Runx3$^{LacZ/LacZ}$ KO mice. Upper panels depict whole mount LacZ staining of E14.5 WT, Kyoto-Runx3$^{LacZ/+}$ and Kyoto-Runx3$^{LacZ/LacZ}$ embryos. Shown are WT and Kyoto-Runx3$^{LacZ/+}$ stained for 48 h and Kyoto-Runx3$^{LacZ/LacZ}$ stained for 16 h. Lower panels depict the corresponding embryos GITs that were excised and stained for LacZ. There is complete absence of positive staining.

no expression was detected in the GIT (Fig 6). In fact, staining of the Kyoto-Runx3$^{LacZ/LacZ}$ GIT was indistinguishable from that of the WT (Runx3$^{+/+}$) littermate embryos. Moreover, increasing the incubation time of isolated GIT with X-gal reagents to 2 days still failed to yield detectable staining in the GIT (Fig 6). This complete lack of LacZ staining in GIT of Kyoto-Runx3$^{LacZ/LacZ}$ embryos stands in direct contrast to the results reported by Li et al that GIT of Kyoto-Runx3$^{LacZ/LacZ}$ KO embryos was darkly stained by LacZ and that this high LacZ expression persists in adult mice (Li et al, 2002).

The consistent outcome of the immunostaining, *in situ* hybridization, RT-qPCR experiment, analyses of Runx3-GFP and R26-reporter (LacZ and tdTomato) mice and our failure to reproduce the results of Li et al (Li et al, 2002) using the Kyoto-Runx3$^{LacZ/LacZ}$ mice demonstrate unequivocally that the expression of Runx3 in GIT is below the detection limit of these highly sensitive assays. Furthermore, the lack of Runx3-Cre mediated reporter expression showed that Runx3 is not even transiently expressed at any stage of epithelial lineage development. A TSG is commonly defined as a gene normally expressed in certain cells, whose loss or inactivation contributes to tumour development in those cells. The evidence presented here demonstrates that *Runx3* does not satisfy the first premise of this definition and hence is highly unlikely to be a bona fide TSG in gastric or colorectal cancers as previously claimed.

It is worth noting, however, that the literature described several examples of TSGs that are not expressed under normal conditions but are activated as a consequence of oncogenic stress (for example p16Ink4a; Bennecke et al, 2010). However, this possibility was not considered by Li et al who attributed their TS claim to loss of the pronounced Runx3 expression they detect in normal GIT Ep. Equally significant, this scenario was not implicated by any, not even a single one, of the 286 published papers that based their research on the correctness of Li et al and went on to postulate loss of Runx3 expression in normal GIT Ep to explain the pathogenesis of various types of cancer. On the contrary, in several epithelial cancers an upregulation of RUNX3 expression was observed and in these cases RUNX3 is considered an oncogene (Carvalho et al, 2005; Lee et al, 2011; Nevadunsky et al, 2009; Salto-Tellez et al, 2006). Potentially related are previous studies reporting that gene alterations in stromal cells such as fibroblasts (Bhowmick et al, 2004; Katajisto et al, 2008) and T cells (Kim et al, 2006) could result in epithelial tumourigenesis. Indeed, Runx3 is expressed in GIT leukocytes and its absence in Runx3$^{-/-}$ mice is associated with colonic inflammation and epithelial

hyperplasia, however, in none of these mice have we (Brenner et al, 2004) or others (Ito et al, 2008) observed an increased incidence of GIT tumours or any other type of tumour. Thus, the notion that Runx3 is a bona fide TSG was based on the claim that it highly expressed in the normal healthy tissue.

As noted before, since the publication of Li et al paper, a large body of literature has been published on the potential involvement of Runx3 in a variety of cancers (Table S1 of Supporting information). There is, however, an important distinction between these previously published papers and the data presented here: None of the previous reports has gone back and carefully examined, using a variety of highly stringent measures, whether Runx3 is actually expressed in the tissue in which it was reported to be expressed. Instead, on the basis of Li et al, the majority of this literature assumed that Runx3 is indeed expressed in the normal GIT and acts as TS in the particular epithelial cancer investigated.

The papers listed in Table S1 of Supporting information can be placed into three distinct categories: (a) Papers, a significant number (145) of which took for granted that the published data was correct and, because Li et al also described *Runx3* DNA methylation in cancer cells, proceeded to analyse the methylation status of the *Runx3* gene in various cancers. However, as was previously noted (Gal-Yam et al, 2008; Keshet et al, 2006; Sproul et al, 2011), several hundred genes undergo methylation in tumour cell genomes, most of which are not expressed in the normal tissue of origin of these cancers. Therefore, a demonstration of promoter methylation, on its own, does not and cannot represent a proof or even a credible indication/suggestion that the methylated gene is a TSG; (b) Papers that are based on Li et al, but tested Runx3 expression in GIT Ep by IHC using poorly characterized (or fully invalidated) Abs that in several cases stained the cell cytoplasm instead of the nucleus. Data in Fig 2A and Fig S1 of Supporting information provide evidence showing that these Abs could not be construed as being specific for Runx3 protein; (c) Papers that used either RT-PCR or well characterized/validated Abs and failed, by either method, to detect Runx3 expression in the Ep of the GIT.

In summary, using seven different stringent measures, we herein provide compelling evidences that not only directly, definitely and unequivocally rule out the possibility that Runx3 is expressed in WT GIT Ep, but also challenge the notion that Runx3 functions in this tissue as TSG. Additionally, the data also call into question the potential function of Runx3 as TSG in other carcinomas.

MATERIALS AND METHODS

Generation of $Runx3^{LacZ/+}$, $Runx3^{P1\text{-}AFP/+}$ and $Runx3^{P2\text{-}EGFP/+}$ KI mice

Generation of $Runx3^{LacZ/+}$ mice was previously described (Levanon et al, 2002). $Runx3^{P1\text{-}AFP/+}$ mice were generated through use of the Gene Bridges recombineering system (Gene Bridges, Heidelberg, Germany) according to the manufacturers instructions. Briefly, a 7.7 kb *SalI* fragment spanning 6 and 1.7 kb regions upstream and downstream, respectively, of the P1-ATG codon was cloned using BAC 145I18 (129S6/SvEvTac from RPCI-22 library, Genome Resource Facility CHORI, Oakland, CA, USA), which spans the entire genomic locus of *Runx3*. This 7.7 kb *SalI* fragment was then recombineered by insertion of an AFP-lox-PGK/*neo*-lox cassette at the initiator ATG of the P1-transcription unit, while leaving the promoter and 5′UTR intact. The targeting fragment was cloned into a Diphtheria Toxin (DTA) pKODT vector (Lexicon Genetics Inc. Texas, USA), which was linearized and electroporated into ES cells (W4—derived from the 129S6/SvEvTac from Taconic). Recombinant G418 resistant ES clones were screened by Southern blotting using 5′ and 3′ probes. *BamHI* digest revealed an 11.8 kb fragment in WT, and 10.8 and 3.7 kb fragments for the targeted allele. Similarly, $Runx3^{P2\text{-}EGFP/+}$ mice were generated using an EcoRV 8.1 kb fragment spanning 3.2 and 4.9 kb regions upstream and downstream, respectively, of the P2-ATG codon, which was cloned from the *Runx3* BAC indicated above. This fragment was modified by insertion of EGFP-lox-PGK/*neo*-lox cassette at the initiator P2-ATG leaving the promoter and 5′UTR intact. Selection of G418 ES clones by Southern blotting employed a *ScaI* digest analysed with 5′ and 3′ probes. DNA of positive recombinant ES cells produced a 12.7 kb fragment for WT, and 5.7 and 10.2 kb fragments for the targeted allele. The $neo^{F/F}$ gene was subsequently removed by mating germline transmitting $Runx3^{P1\text{-}AFP/+}$ and $Runx3^{P2\text{-}EGFP/+}$ KI mice with transgenic Pgk-Cre mice. Both strains were then backcrossed onto ICR mice. All experiments involving mice were approved by the Institutional Animal Care and Use Committee (IACUC) of the Weizmann Institute.

Generation of $Runx3^{Cre}$ mice

$Runx3^{Cre}$ mice were generated using recombineering as detailed above. A 9 kb *SalI* genomic fragment spanning 3.5 and 5.5 kb regions upstream and downstream, respectively, of *Runx3* exon 4 was cloned from the *Runx3* BAC described above. This fragment was then modified by recombineering using an EGFP-Cre cassette (pBS592, Addgene, USA). This EGFP-Cre cassette, which consisted of EGFP-Cre-CSF-PolyA-frt-Pgk/neo-frt was inserted in-frame into exon 4 (into the *SmaI* site) creating Runx3-EGFP-Cre fused protein. We chose the *SmaI* site, because it was utilized by Li et al (Li et al, 2002) to create the Kyoto-$Runx3^{LacZ/LacZ}$ mice, which gave rise to the strong LacZ stained GIT reported in their paper Fig 1E (Li et al, 2002). The EGFP-Cre cassette was selected because it combines the advantage of a GFP reporter and more importantly, when used as EGFP-Cre fusion protein was shown to be efficient in the excision of LoxP-flanked genomic fragments (Le et al, 1999). The targeting fragment was electroporated into ES cells (129X1/SvJ x 129S1) followed by selection of G418 ES clones using Southern blotting of *ScaI* digest analysed with 5′ and 3′ probes. DNA of positive recombinant ES cells produced an 11.1 kb fragment for WT, and 9.3 and 5.9 kb fragments for the targeted allele.

The R26-$stop^{Flox}$-LacZ and R26-$stop^{Flox}$-tdTomato reporter mouse strains

R26-$stop^{Flox}$-LacZ mice were obtained from the Jackson Laboratory (strain name B6; 129S4-*Gt(ROSA)26Sor*^{tm1Sor}/J; stock No. 003309). *Cre* expression in these mice results in the removal of a *loxP*-flanked DNA segment (STOP cassette) that prevents expression of a *lacZ* gene. When crossed with a *cre* expressing mouse strain, *lacZ* is expressed in cells/tissues where *cre* is expressed. R26-$stop^{Flox}$-tdTomato mice were also obtained from the Jackson Laboratory (strain name

The paper explained

PROBLEM:

Tumour suppressor genes (TSG) play an important role in protecting normal tissues against cancer development. To function as a tumour suppressor (TS), a gene must be expressed in cells of the normal tissue, while loss of its expression should give the cell a spur to growth that may potentially lead to cancer. Almost 10 years ago it was reported by Li et al (2002) that Runx3 is an important TSG in gastrointestinal tract (GIT) epithelium (Ep), based on their finding of its high expression in GIT Ep of $Runx3^{LacZ/LacZ}$ mouse embryos. Subsequently, more than 280 papers have been published, which based their research on the Li et al 2002 finding, invoking the loss of Runx3 activity to explain the pathogenesis of one or another type of human cancer. In these papers, the correctness of the 2002 report that *Runx3* is indeed a TSG has always been assumed. Here, we re-examined in great detail and using a variety of highly sensitive genetic, biochemical and immunohistochemical techniques the most critical question: Is Runx3 indeed expressed in normal GIT Ep?

RESULTS:

Employing a variety of biochemical and genetic techniques, including analysis of Runx3-GFP and R26LacZ/Runx3Cre or R26tdTomato/Runx3Cre reporter strains, we readily detected Runx3 in GIT-embedded leukocytes as well as in various other known Runx3 expressing cells and organs. None of these approaches, however, revealed detectable Runx3 levels in GIT Ep. Moreover, the results of the R26LacZ/Runx3Cre and R26tdTomato/Runx3Cre reporter analysis demonstrated that Runx3 was not even transiently expressed at any time during epithelial lineage development. Finally, a rigorous analysis of the original Kyoto-$Runx3^{LacZ/LacZ}$ mice used in the original Li et al study failed to reproduce the reported LacZ staining in the GIT.

IMPACT:

The lack of evidence for Runx3 expression in normal GIT Ep at any stage of normal GIT development presents a serious challenge to the published data and undermines the notion that Runx3 is a TS involved in cancer pathogenesis.

B6.Cg-*Gt(ROSA)26Sor*$^{tm14(CAG-tdTomato)Hze}$/J; stock No. 007914). These mice harbour a targeted mutation of the *Gt(ROSA)26Sor* locus with a *loxP*-flanked STOP cassette preventing transcription driven by the highly active CMV early enhancer/chicken β actin (CAG) promoter, which then mediate the expression of cells/tissues specific red fluorescent protein variant (tdTomato). These two mouse strains are used here as Runx3-Cre reporters that express either LacZ or tdTomato following Runx3-mediated expression of Cre-recombinase. $Runx3^{Cre}$ mice crossed onto the R26-$stop^{Flox}$-LacZ or R26-$stop^{Flox}$-tdTomato reporter mouse strains, exhibited the characteristic Runx3 expression pattern with no expression in the GIT, whereas, when crossed onto the general deleter strain Pgk-Cre, the R26-$stop^{Flox}$-LacZ or R26-$stop^{Flox}$-tdTomato displayed ubiquitous blue staining or red fluorescence, respectively, including strong staining in the GIT.

Analysis of Runx3 expression

Monitoring Runx3 expression via Runx3- LacZ or -GFP

X-Gal staining was performed as previously described (Levanon et al, 2001) using a standard procedure (Hames & Higgins, 1993). GFP expression was viewed in whole mount embryos using a fluorescence stereomicroscope (Leica MZ16F) equipped with GFP filter sets. AFP and EGFP are variants of GFP recognized by the commercially available anti-GFP Abs indicated below.

Immunohistochemistry (IHC) and immunofluorescence

IHC and immunofluorescence were conducted using paraffin sections as previously described (Levanon et al, 2002). Runx3 was detected by Vectastain kit (Vector Laboratories Burlingame, CA, USA) or, when applicable, by the MOM kit for monoclonal Abs (Vector Laboratories Burlingame). The following Abs were used: affinity purified rabbit anti-Runx1 (1:100 dilution) produced in-house; polyclonal rabbit anti-Runx3 'poly-G' (1:1000; Levanon et al, 2002, 2001); monoclonal anti-Runx3 Abs 'Mono-G' (1:200) raised in-house (in collaboration with RCMDT, Russian Research Center, Moscow, Russia), against the Runx3 peptide—TPSTPSPRGSLSTTSHF; rabbit anti-RUNX3 'Poly-SA' (1:1000) produced by Sylvia Arber Biozentrum, Basel, Switzerland (Kramer et al, 2006); rabbit anti-Runx3 Abs 'Pep-J' (1:1000) raised against the Runx3 peptide—AQATAGPGGRTRPEVRS by Joriene de Nooij in the laboratory of Tom Jessell New York, NY, USA (Kramer et al, 2006); anti-Runx3 Abs 'GS' raised by GeneScript, CRO (Piscataway, NJ, USA), against the same peptide used by Joriene de Nooij; anti-AML2/Runx3 rabbit polyclonal (1:200) ACTIVE MOTIF (Carlsbad, CA USA) and monoclonal anti-Runx3 Abs R3-1E10, R3-3F12 and R3-8C9 (1:200; Fig S1A–C of Supporting information) raised in the laboratory of Yoshiaki Ito against portions of Runx3 and subsequently characterized (Ito et al, 2009); and goat polyclonal Abs against GFP (biotin) Ab-6658 (1:200) Abcam, Cambridge, UK.

Radioactive RNA in situ hybridizations

Radioactive RNA in situ hybridizations of *Runx3* or *Runx1* mRNAs were performed as previously described (Brenner et al, 2004) using ^{35}S-labeled RNA probes. The *Runx1* probe spanned 650 bp of exon 6 between nucleotides 1114–1765 in GenBank accession No. D13802. The *Runx3* probe spanned 769 bp of exon 6 between nucleotides 1035–1804 in GenBank accession #AF155880.

Flow cytometry

This was performed using single cell suspensions of embryonic or adult GIT Ep derived from $Runx3^{P1\text{-}AFP/P2\text{-}EGFP}$, R26-LacZ/$Runx3^{Cre}$ or R26-tdTomato/$Runx3^{Cre}$ reporter mouse strains. For $Runx3^{P1\text{-}AFP/P2\text{-}EGFP}$, colon and cecum of adult WT and reporter mice

were removed, opened longitudinally, washed in PBS, cut into 0.5 cm pieces and incubated twice for 20 min at 37°C in Hanks balanced salt solution (HBSS) containing 2 mM EDTA, 1 mM DTT and 5% FCS. The two suspensions were combined, passed through a 100 μm cell strainer and washed twice in FACS buffer (PBS containing 5% FCS, 1 mM EDTA and 0.05% Na azide). Preparations of GIT Ep contained a substantial number of Runx3 expressing IELs, as documented in Fig. 2. Cells were immunostained with anti EpCAM (BD Biosciences, USA) in combination with anti-rat IgG Cy5 (Jackson ImmunoResearch) or CD45-APC (BD Biosciences). The GITs (see Fig 5B, C and F) and thymi of E16.5 R26-LacZ/Runx3^{Cre} or R26-tdTomato/Runx3^{Cre} embryos were removed and single cell suspensions of thymocytes or intestinal Ep were prepared. The cells obtained from R26-LacZ/Runx3^{Cre} embryos were loaded with FDG (Molecular Probes; Eugene, OR, USA) to detect LacZ-positive cells (North et al, 2004), and thymocytes and epithelial cells from both R26-LacZ/Runx3^{Cre} or R26-tdTomato/Runx3^{Cre} were immunostained with anti-CD45 (e-Bioscience, San-Diego, CA, USA) or anti-EpCAM (BD Biosciences) in combination with anti-rat IgG Cy5 (Jackson ImmunoResearch). FACS analysis was performed using BD LSRII (Becton Dickenson, USA) and analysed by Flowjo software.

Reverse transcription quantitative real-time PCR (RT-qPCR)

RNA was prepared using RNeasy micro RNA preparation kits (Qiagen, Hilden, BRD), according to manufacturer's instructions. All samples had OD260/280 ≥1.9 and OD 260/230 ≥1.0. Minimum two RNA preps were done per cell type (*i.e.* EpCAM$^+$and CD45$^+$NK). Reverse transcription was carried out using SuperScript II (Invitrogen, Carlsbad, CA, USA) and random hexamer primers, template concentration was in the linear range of amplification. Endogenous control assays gave statistically stable expression, and normalization factors were calculated via geometric averaging of the two genes' expression levels using BestKeeper software (Pfaffl et al, 2004). Quantification was calculated relative to the lowest-expressing sample as calibrator using random pairwise allocation, and statistical significance using Taylor's series via REST 384 software (Pfaffl et al, 2002).

TaqMan assays of Runx3, HPRT1 and PBGD (Runx3-Mm00490666_M1; HPRT1-Mm00446968_M1; PBGD-Mm00660262_G1) were purchased from Applied Biosystems (ABI), and were confirmed 100% efficient under in-house conditions. The HPRT1 and PBGD endogenous control assays were chosen from different protein families with differing biological functions, to ensure that normalization would be stable and were confirmed to give signal within the range similar to actual samples. Reactions were run with TaqMan Gene Expression Master Mix (ABI #4369016) in a Roche LC480 realtime PCR instrument under two-step absolute quantification with extended denaturation times and T_m 61°C. Minimum three technical repeats of each sample were run. All assays gave SD < 0.35 for cycle thresholds (Ct) values over all samples.

Author contributions

DL, KRB, AP and YG designed the experiments; DL, YB, VN, KRB, AP, RE, JL and OB performed the experiments; DL, KRB, AP, OB and YG analysed the data; DL, JL and YG wrote the paper.

Acknowledgements

We thank Nancy Speck for the Runx1$^{LacZ/+}$ mice, Silvia Arber for the poly-SA anti-Runx3 Abs, Joriene de Nooij from the Jessell lab for the pep-J anti-Runx3 Abs and Yoshiaki Ito for the R3-1E10, R3-3F12 and R3-8C9 monoclonal anti-Runx3 Abs as well as for the Kyoto-Runx3$^{LacZ/LacZ}$ mice. We acknowledge the help of Rafi Saka, Judith Chermesh and Ofira Higfa in animal husbandry, Golda Damari, Sima Peretz and Alina Maizenberg in microinjections and Rebecca Hafner in ES cells selection. This study was supported by grants from Israel Science Foundation (ISF) individual grant and the Bio-Med program and by the Commission of the EU (AnEUploidy).

Supporting information is available at EMBO Molecular Medicine online.

The authors declare that they have no conflict of interest.

References

Avraham KB, Levanon D, Negreanu V, Bernstein Y, Groner Y, Copeland NG, Jenkins NA (1995) Mapping of the mouse homolog of the human runt domain gene, AML2, to the distal region of mouse chromosome 4. Genomics 25: 603-605

Bangsow C, Rubins N, Glusman G, Bernstein Y, Negreanu V, Goldenberg D, Lotem J, Ben-Asher E, Lancet D, Levanon D, *et al* (2001) The RUNX3 gene—sequence, structure and regulated expression. Gene 279: 221-232

Bennecke M, Kriegl L, Bajbouj M, Retzlaff K, Robine S, Jung A, Arkan MC, Kirchner T, Greten FR (2010) Ink4a/Arf and oncogene-induced senescence prevent tumor progression during alternative colorectal tumorigenesis. Cancer Cell 18: 135-146

Bhowmick NA, Neilson EG, Moses HL (2004) Stromal fibroblasts in cancer initiation and progression. Nature 432: 332-337

Brenner O, Levanon D, Negreanu V, Golubkov O, Fainaru O, Woolf E, Groner Y (2004) Loss of Runx3 function in leukocytes is associated with spontaneously developed colitis and gastric mucosal hyperplasia. Proc Natl Acad Sci USA 101: 16016-16021

Carvalho R, Milne AN, Polak M, Corver WE, Offerhaus GJ, Weterman MA (2005) Exclusion of RUNX3 as a tumour-suppressor gene in early-onset gastric carcinomas. Oncogene 24: 8252-8258

Chen CL, Broom DC, Liu Y, de Nooij JC, Li Z, Cen C, Samad OA, Jessell TM, Woolf CJ, Ma Q (2006) Runx1 determines nociceptive sensory neuron phenotype and is required for thermal and neuropathic pain. Neuron 49: 365-377

Collins A, Littman DR, Taniuchi I (2009) RUNX proteins in transcription factor networks that regulate T-cell lineage choice. Nat Rev Immunol 9: 106-115

DaCosta RS, Andersson H, Cirocco M, Marcon NE, Wilson BC (2005) Autofluorescence characterisation of isolated whole crypts and primary cultured human epithelial cells from normal, hyperplastic, and adenomatous colonic mucosa. J Clin Pathol 58: 766-774

Gal-Yam EN, Egger G, Iniguez L, Holster H, Einarsson S, Zhang X, Lin JC, Liang G, Jones PA, Tanay A (2008) Frequent switching of Polycomb repressive marks and DNA hypermethylation in the PC3 prostate cancer cell line. Proc Natl Acad Sci USA 105: 12979-12984

Hames BD, Higgins SJ (1993) *Gene Transcription—A Practical Approach*. New York, IRL Press at Oxford University Press.

Inoue K, Ozaki S, Shiga T, Ito K, Masuda T, Okado N, Iseda T, Kawaguchi S, Ogawa M, Bae SC, *et al* (2002) Runx3 controls the axonal projection of proprioceptive dorsal root ganglion neurons. Nat Neurosci 5: 946-954

Ito Y (2008) RUNX genes in development and cancer: regulation of viral gene expression and the discovery of RUNX family genes. Adv Cancer Res 99: 33-76

Ito K, Lim AC, Salto-Tellez M, Motoda L, Osato M, Chuang LS, Lee CW, Voon DC, Koo JK, Wang H, *et al* (2008) RUNX3 attenuates beta-catenin/T cell factors in intestinal tumorigenesis. Cancer Cell 14: 226-237

Ito K, Inoue KI, Bae SC, Ito Y (2009) Runx3 expression in gastrointestinal tract epithelium: resolving the controversy. Oncogene 28: 1379-1384

Jung S, Aliberti J, Graemmel P, Sunshine MJ, Kreutzberg GW, Sher A, Littman DR (2000) Analysis of fractalkine receptor CX(3)CR1 function by targeted deletion and green fluorescent protein reporter gene insertion. Mol Cell Biol 20: 4106-4114

Katajisto P, Vaahtomeri K, Ekman N, Ventela E, Ristimaki A, Bardeesy N, Feil R, DePinho RA, Makela TP (2008) LKB1 signaling in mesenchymal cells required for suppression of gastrointestinal polyposis. Nat Genet 40: 455-459

Keshet I, Schlesinger Y, Farkash S, Rand E, Hecht M, Segal E, Pikarski E, Young RA, Niveleau A, Cedar H, *et al* (2006) Evidence for an instructive mechanism of *de novo* methylation in cancer cells. Nat Genet 38: 149-153

Kim BG, Li C, Qiao W, Mamura M, Kasprzak B, Anver M, Wolfraim L, Hong S, Mushinski E, Potter M, *et al* (2006) Smad4 signalling in T cells is required for suppression of gastrointestinal cancer. Nature 441: 1015-1019

Kramer I, Sigrist M, de Nooij JC, Taniuchi I, Jessell TM, Arber S (2006) A role for Runx transcription factor signaling in dorsal root ganglion sensory neuron diversification. Neuron 49: 379-393

Le Y, Miller JL, Sauer B (1999) GFPcre fusion vectors with enhanced expression. Anal Biochem 270: 334-336

Lee CW, Chuang LS, Kimura S, Lai SK, Ong CW, Yan B, Salto-Tellez M, Choolani M, Ito Y (2011) RUNX3 functions as an oncogene in ovarian cancer. Gynecol Oncol 122: 410-417

Levanon D, Groner Y (2004) Structure and regulated expression of mammalian RUNX genes. Oncogene 23: 4211-4219

Levanon D, Groner Y (2009) Runx3-deficient mouse strains circa 2008: resemblance and dissimilarity. Blood Cells Mol Dis 43: 1-5

Levanon D, Negreanu V, Bernstein Y, Bar-Am I, Avivi L, Groner Y (1994) AML1, AML2, and AML3, the human members of the runt domain gene-family: cDNA structure, expression, and chromosomal localization. Genomics 23: 425-432

Levanon D, Brenner O, Negreanu V, Bettoun D, Woolf E, Eilam R, Lotem J, Gat U, Otto F, Speck N, *et al* (2001) Spatial and temporal expression pattern of Runx3 (Aml2) and Runx1 (Aml1) indicates non-redundant functions during mouse embryogenesis. Mech Dev 109: 413-417

Levanon D, Bettoun D, Harris-Cerruti C, Woolf E, Negreanu V, Eilam R, Bernstein Y, Goldenberg D, Xiao C, Fliegauf M, *et al* (2002) The Runx3 transcription factor regulates development and survival of TrkC dorsal root ganglia neurons. EMBO J 21: 3454-3463

Levanon D, Brenner O, Otto F, Groner Y (2003) Runx3 knockouts and stomach cancer. EMBO Rep 4: 560-564

Li QL, Ito K, Sakakura C, Fukamachi H, Inoue K, Chi XZ, Lee KY, Nomura S, Lee CW, Han SB, *et al* (2002) Causal relationship between the loss of RUNX3 expression and gastric cancer. Cell 109: 113-124

Nevadunsky NS, Barbieri JS, Kwong J, Merritt MA, Welch WR, Berkowitz RS, Mok SC (2009) RUNX3 protein is overexpressed in human epithelial ovarian cancer. Gynecol Oncol 112: 325-330

North T, Gu TL, Stacy T, Wang Q, Howard L, Binder M, Marin-Padilla M, Speck NA (1999) Cbfa2 is required for the formation of intra-aortic hematopoietic clusters. Development 126: 2563-2575

North TE, Stacy T, Matheny CJ, Speck NA, de Bruijn MF (2004) Runx1 is expressed in adult mouse hematopoietic stem cells and differentiating myeloid and lymphoid cells, but not in maturing erythroid cells. Stem Cells 22: 158-168

Pfaffl MW, Horgan GW, Dempfle L (2002) Relative expression software tool (REST) for group-wise comparison and statistical analysis of relative expression results in real-time PCR. Nucleic Acids Res 30: e36

Pfaffl MW, Tichopad A, Prgomet C, Neuvians TP (2004) Determination of stable housekeeping genes, differentially regulated target genes and sample integrity: BestKeeper—Excel-based tool using pair-wise correlations. Biotechnol Lett 26: 509-515

Pozner A, Lotem J, Xiao C, Goldenberg D, Brenner O, Negreanu V, Levanon D, Groner Y (2007) Developmentally regulated promoter-switch transcriptionally controls Runx1 function during embryonic hematopoiesis. BMC Dev Biol 7: 84

Salto-Tellez M, Peh BK, Ito K, Tan SH, Chong PY, Han HC, Tada K, Ong WY, Soong R, Voon DC, *et al* (2006) RUNX3 protein is overexpressed in human basal cell carcinomas. Oncogene 25: 7646-7649

Soriano P (1999) Generalized lacZ expression with the ROSA26 Cre reporter strain. Nat Genet 21: 70-71

Sproul D, Nestor C, Culley J, Dickson JH, Dixon JM, Harrison DJ, Meehan RR, Sims AH, Ramsahoye BH (2011) Transcriptionally repressed genes become aberrantly methylated and distinguish tumors of different lineages in breast cancer. Proc Natl Acad Sci USA 108: 4364-4369

Srinivas S, Watanabe T, Lin CS, William CM, Tanabe Y, Jessell TM, Costantini F (2001) Cre reporter strains produced by targeted insertion of EYFP and ECFP into the ROSA26 locus. BMC Dev Biol 1: 4

Woolf E, Xiao C, Fainaru O, Lotem J, Rosen D, Negreanu V, Bernstein Y, Goldenberg D, Brenner O, Berke G, *et al* (2003) Runx3 and Runx1 are required for CD8 T cell development during thymopoiesis. Proc Natl Acad Sci USA 100: 7731-7736

Yoshida CA, Yamamoto H, Fujita T, Furuichi T, Ito K, Inoue K, Yamana K, Zanma A, Takada K, Ito Y, *et al* (2004) Runx2 and Runx3 are essential for chondrocyte maturation, and Runx2 regulates limb growth through induction of Indian hedgehog. Genes Dev 18: 952-963

